Tight binding description on the band gap opening of pyrene-dispersed graphene

Dong-Meng Chen,[ab] Prathamesh M. Shenai[a] and Yang Zhao*[a]

Received 17th June 2010, Accepted 12th October 2010
DOI: 10.1039/c0cp00909a

Opening up a band gap in graphene holds a crucial significance in the realization of graphene-based electronics. Doping with organic molecules to alter the electronic properties of graphene is perceived as an effective band gap engineering approach. Using the tight binding model, we examined the band gap opening of monolayer graphene due to the adsorption of pyrene molecules on both of its sides. It was found that the breakdown of the sublattice symmetry in pyrene-dispersed graphene leads to a band gap of $\sim$10 meV.

1. Introduction

Graphene is a two-dimensional network of carbon atoms arranged in a honeycomb lattice. Although for a long time it has been known that graphite is structured by the stacking of individual graphene sheets, research focusing on graphene gathered momentum only after breakthroughs in its first successful isolation in 2004.[1,2] The strong σ bond between two carbon atoms of graphene by the virtue of sp^2 hybridization accounts for its remarkable structural strength and flexibility.[3] In monolayer graphene, the sp^2 hybridization results in the formation of a σ bond with a filled shell between carbon atoms, leading to a deep valence band. The half-filled π band is constructed by the unaffected p-orbital, which is perpendicular to its planar structure. The dispersion of π and π* electronic bands is crucial for the formation of the band gap in graphene. Its electronic properties are influenced by a significant structural flexibility. In a pristine graphene layer, a primitive unit cell contains two carbon atoms, the *i* and *j* sublattice (Fig. 1a). The π and π* bands intersect at two Dirac points, *K* and *K′*, in the corresponding reciprocal space (Fig. 1b). As the two bands are degenerate at the Dirac points, graphene is a zero-gap semiconductor with a massless Dirac spectrum.[4]

Its unique planar morphology and ballistic charge carrier transport properties make graphene a highly attractive candidate for laying out nanoelectronic circuitry.[5] However, in order to tap this potential in various electronic device applications, the presence of a band gap is indispensable. Different theoretical approaches have been proposed to introduce a band gap into graphene. The size reduction of graphene to under 10 nm, forming narrow strips or nanoribbons, leads to quantum confinement effects that open up a distinct band gap.[6] Although dependable, this approach suffers from the extreme sensitivity of the band gap opening towards the nanoribbon width, edge structures and chemical decoration. Removal of translational symmetry is one of the most commonly used approaches to lift the degeneracy exhibited by pristine graphene. The band gap is created when the two crystallographically-equivalent atoms in the primitive unit cell become inequivalent, *i.e.*, when the sublattice symmetry is broken. Experimental efforts to introduce a band gap in pristine graphene include growing the graphene on certain substrates,[7,8] applying an external electric bias,[9,10] shaping graphene in the form of narrow ribbons[6] and perforating graphene, leading to a "graphene nano-mesh".[11] Furthermore, in the field effect transistor (FET) set-up based on bilayer graphene, a simple device geometry change, such as the use of a dual gate instead of a single gate, was also shown to exhibit a band gap opening of up to 0.25 eV.[10] These techniques induce changes in the electronic properties of graphene without any direct chemical modification.

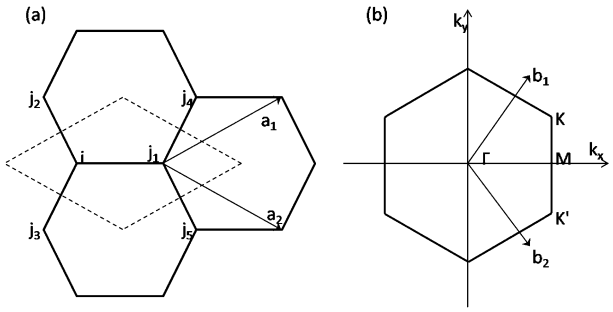

Fig. 1 (a) The pristine graphene unit cell. $\vec{a}_1$, $\vec{a}_2$ are the unit cell vectors, and j_1, j_2, j_3 are the three nearest-neighbor atoms for *i*. j_4, j_5 represent the second-nearest-neighbor. The dashed lines denote the primitive unit cell. (b) The first Brillouin zone. Γ is the center of the cell. *K* and *K′* are the corners of the first Brillouin zone (Dirac points), and *M* is the center of the edge. The energy spectra are obtained along Γ, *K* and *M*[4].

Another route involves exploiting the reactivity of graphene to alter its electronic structure *via* the chemical adsorption of various species. Molecular decoration of graphene or the introduction of nanoholes in pristine graphene have been shown to bring about the desired removal of translational symmetry, thus opening the band gap.[12–14] Complete hydrogenation transforms graphene into graphane, which has a very large band gap.[15] However, a controlled modulation of the band gap of graphene was shown to be possible *via* partial hydrogenation[16–18] or even *via* patterned hydrogen

[a] *School of Materials Science and Engineering, Nanyang Technological University, Singapore 639789, Singapore. E-mail: YZhao@ntu.edu.sg*
[b] *College of Physics Science and Technology, China University of Petroleum, Dongying 257061, China*

adsorption.[19] Various other organic molecules, especially those with large aromatic ring structures, have also been studied in conjunction with their physical or chemical adsorption on graphene.[20–23] In a few studies, a different approach by introducing holes into graphene to form anti-dot lattices has also been shown to be an effective way of inducing a band gap *via* quantum confinement effects.[24,25]

Certain graphite intercalated compounds (GIC) have been studied in relation to their high temperature superconductivity.[26,27] It has also emerged that the electronic structure of GICs resembles to that of doped graphene. Recent studies on CaC_6 and other XC_6 intercalated compounds indicate the prominent role of graphene in inducting superconductivity in them.[26,28,29] Ca atoms are interdispersed between adjacent graphene sheets in CaC_6 and affect both the inter-sheet distance as well as C–C bond lengths in the graphene plane. Periodic modulations in the graphene sheets in the vicinity of Ca atoms can be described by changes in the charge-transfer integral between a given pair of C-atoms, an approach akin to what we have employed in the current work on pyrene-adsorbed graphene.

In this paper, we investigate the effect of molecular decoration with the physical adsorption of pyrene molecules on the graphene band gap. No chemical bonding or direct charge-transfer between graphene and pyrene molecules is taken into account. We characterize the electronic bandstructure of graphene using the tight-binding model. Within the extent of the current work, it has been shown that a small but distinct band gap can be opened up in graphene resulting from the broken sub-lattice symmetry.

The rest of the paper is organized as below. Section 2 describes the tight-binding model used for calculating the band structure of pyrene-adsorbed graphene in different configurations of bond length distortions. Results are presented and discussed in detail in the section 3. The effects of on-site energy and the change in the charge-transfer integral in modifying the graphene band-structure are detailed. Results of the present work are compared with some literature reports examining the band gap opening behavior in graphene. Conclusions are drawn in final section 4.

2. Details of the model and methodology

In this paper, it is assumed that there are two pyrene molecules per 6 × 6 unit cells of graphene, one molecule being on the either side of the graphene. The graphene monolayer is sandwiched between the pyrene molecules in a configuration such that one of the C atoms in the pyrene molecules is located over the center of the hexagon in the graphene while the other assumes a position directly above a C atom of graphene, as illustrated in Fig. 2. DFT calculations are performed using the DMol3 package with all the electrons considered, and with the use of the GGA (PBE) and DNP basis sets.

On the pyrene-dispersed graphene, significant sublattice symmetry breaking is revealed in the DFT results, as exhibited by the changes in C–C bond lengths within the graphene layer. The C–C bond length in pristine graphene is 1.420 Å. However, the adsorption of pyrene molecules leads to

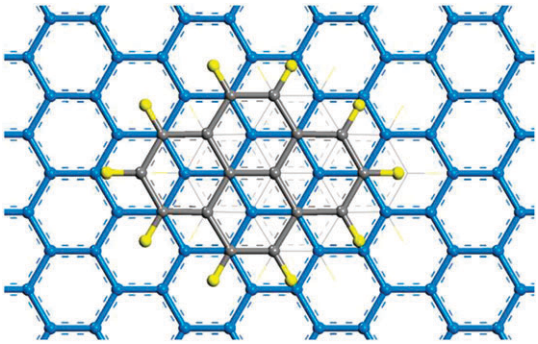

Fig. 2 The orientation of pyrene-dispersed graphene: the blue molecule is graphene and the gray molecule is pyrene, with a spacing of 3.4 Å. The other pyrene molecule is beneath the graphene layer. The yellow atoms are hydrogens.

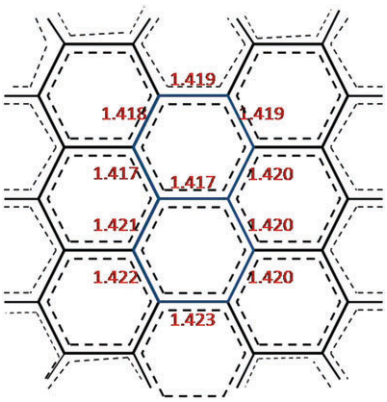

Fig. 3 The carbon–carbon bond lengths of graphene after the adsorption of pyrene molecules.

a significant coupling between pyrene and graphene, thereby making the six bond lengths in the honeycomb structure inequivalent. We observe a maximum variation of ~0.2% in the bond lengths (Fig. 3) from the equilibrium distance of 1.42 Å. We expect that such a variation that breaks the sub-lattice symmetry will eventually lead to the formation of a band gap in graphene.

Using the *ab initio* results as a rough guide, we assume four different forms of distortions that can be induced in the graphene as a result of its coupling with pyrene. These forms are designated as d1, d2, d3 and d4, as shown in Fig. 4. Those C–C bonds that were observed to undergo contraction are represented by solid black lines. On the other hand, the red solid lines depict bonds that undergo extension. These four distortion configurations are used to simulate the effects of disorder on the band structure of graphene on account of C–C bond distortions.

The tight-binding model is employed to calculate the band structure of the pyrene-dispersed graphene. The Columbic repulsion breaks the symmetry of graphene, which is reflected as the inequivalent bond lengths in the graphene supercell. The lattice vectors of the primitive unit cell in pristine graphene can be written as $\mathbf{a_1} = a(\sqrt{3}/2,\ 1/2)$ and $\mathbf{a_2} = a(\sqrt{3}/2,\ -1/2)$, where a is the lattice constant and equals 1.42 Å × $\sqrt{3}$ = 2.46 Å. For a given C-atom, its

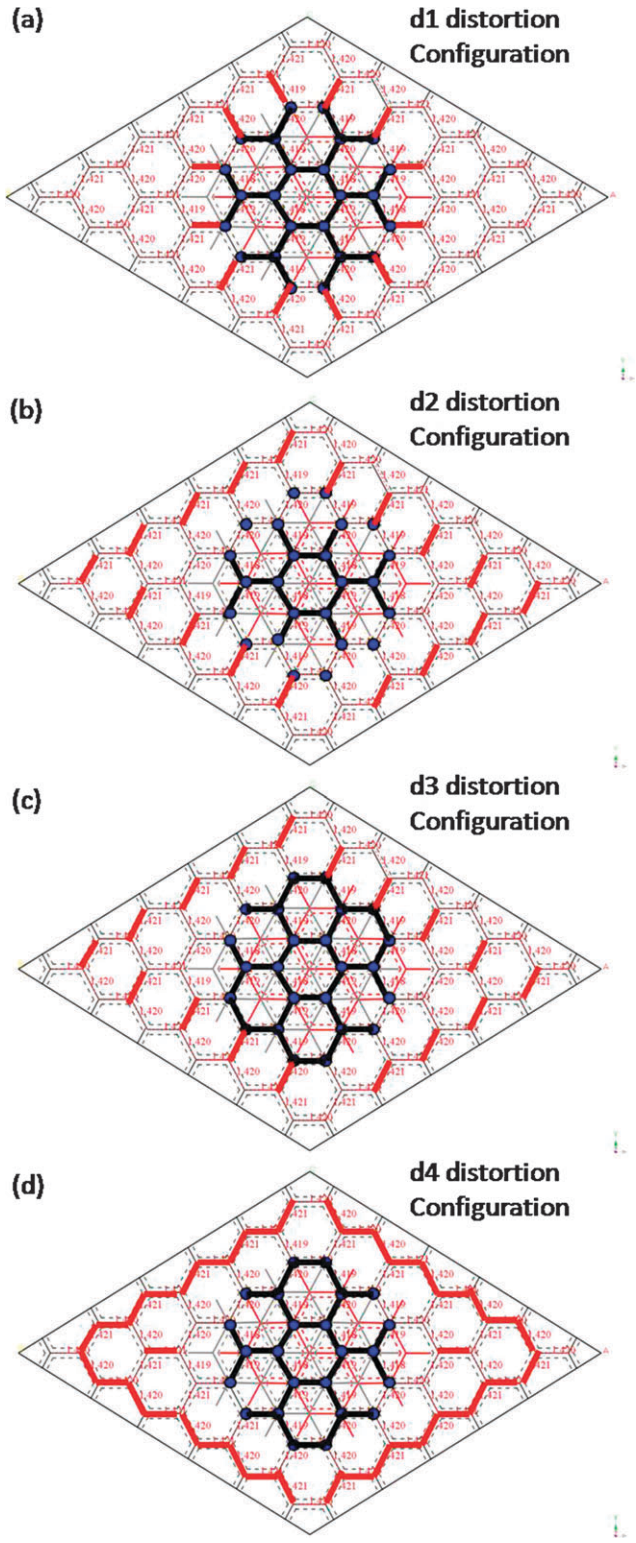

Fig. 4 Different assumed forms of distortion of graphene due to the adsorption of pyrene designated as d1 (a), d2 (b), d3 (c) and d4 (d). Solid black lines denote bond length shortening while solid red lines represent bonds that undergo extension. Blue circles represent the atoms of the graphene layer sandwiched by the pyrene molecules.

three nearest-neighbors can be specified as $\mathbf{j_1} = a(1/\sqrt{3},\ 0)$, $\mathbf{j_2} = a(-1/2\sqrt{3},\ 1/2)$ and $\mathbf{j_3} = a(-1/2\sqrt{3},\ -1/2)$.

Furthermore, using an adopted approach, the tight-binding Hamiltonian of pyrene-dispersed graphene is written as[24,25]

$$H = \sum_{\mathbf{R},\mathbf{m}} \varepsilon_{\mathbf{R},\mathbf{m}} c^{\dagger}_{\mathbf{R}+\mathbf{d_m}} c_{\mathbf{R}+\mathbf{d_m}} - \sum_{\langle \mathbf{R},\mathbf{m},\delta \rangle} t_{\mathbf{R}+\mathbf{d_m}+\delta,\mathbf{R}+\mathbf{d_m}} \left(c^{\dagger}_{\mathbf{R}+\mathbf{d_m}+\delta} c_{\mathbf{R}+\mathbf{d_m}} + Hc \right) \quad (1)$$

where a set of $\mathbf{R}$ denotes unit cells and $\mathbf{d_m}$ (m = 1, …, N_c) denote the C atoms' positions in a given unit cell. For a C atom at position $\mathbf{R} + \mathbf{d_m}$, δ represents its nearest neighbors. N_c is the number of C atoms in one unit cell, and $N_c = 72$ for pyrene-dispersed graphene. $t_{\mathbf{R}+\mathbf{d_m}+\delta,\mathbf{R}+\mathbf{d_m}}$ is the hopping integral for electrons to jump from site $\mathbf{R}+\mathbf{d_m}$ to site $\mathbf{R}+\mathbf{d_m}+\delta$, and its value fluctuates around the transfer integral for pristine graphene ($t \approx 2.8$ eV). Furthermore, the C-atoms located in the region sandwiched by pyrene molecules have a modified on-site energy, P, due to static electric potentials. For the purpose of calculations, we have suitably assumed certain values of $\varepsilon_{\mathbf{R}+\mathbf{d_m}}$.

In the Hamiltonian expression of eqn (1), $\varepsilon_{\mathbf{R}+\mathbf{d_m}}$ is written as:

$$\varepsilon_{\mathbf{R}+\mathbf{d_m}} = \begin{cases} \varepsilon_{2p}, & i \text{ is not sandwiched by pyrene} \\ \varepsilon_{PA}, & i \text{ is sandwiched by pyrene.} \end{cases} \quad (2)$$

When atoms are not sandwiched by the pyrene, ε_i gives the orbital energy of the $2p$ level, ε_{2p}, which is set to be zero here for simplicity. Sites on the graphene sheet sandwiched by pyrene molecules will have a higher energy, ε_{PA}, due to the static electric potential between pyrene and graphene.

In our model, the Bloch wave functions corresponding to the energy eigenvalues $\varepsilon_n(\mathbf{k})$ (n is the band index) are given by $\psi_{nk}(\mathbf{r}) = \sum_{\mathbf{m}} \mathbf{a_m^{n,k}}\ \boldsymbol{\phi}_{\mathbf{mk}}(\mathbf{r})$, where $\phi_{mk}(\mathbf{r}) = \mathbf{N^{-1/2}} \sum_{\mathbf{R}} \mathbf{e^{ik\cdot R}} \varphi(\mathbf{r}-\mathbf{R}-\mathbf{d_m})$ and $\varphi(\mathbf{r}-\mathbf{R}-\mathbf{d_m})$ is the $2p_z$ orbital of a C atom at $\mathbf{R}+\mathbf{d_m}$. As an approximation, we have neglected the overlap of the $2p_z$ orbitals on different atoms.

3. Results and discussion

The eigenvalues $E_n(\mathbf{k})$ are obtained by diagonalizing the Hamiltonian H. The opening of the energy band gap due to the induced symmetry breaking is evident. Shrinkage of the Brillouin zone due to the selection of the supercell leads to a band-folding effect, and the energy band-gap appears at or close to the Γ point rather than the K point. The band structure of the pyrene-adsorbed graphene is calculated under the effects of modification in the hopping integral (Δt) and the on-site energy (P). Under various conditions, we have found the band gap opening to occur for all the four distortion configurations considered here. The magnitude of the band gap depends upon the values of Δt and P.

We first consider the band gap opening under the influence of increase in on-site energy P while Δt is set to zero. This implies no bond length deviations for the pyrene-dispersed graphene (as compared to pristine graphene) are considered. Fig. 5 exhibits a non-linear increase in the band gap resulting from an increase in P for graphene. The on-site energy arises from Coulombic repulsive interactions between the electrons of C-atoms of pyrene molecules and those of the atoms of graphene sandwiched by pyrene.

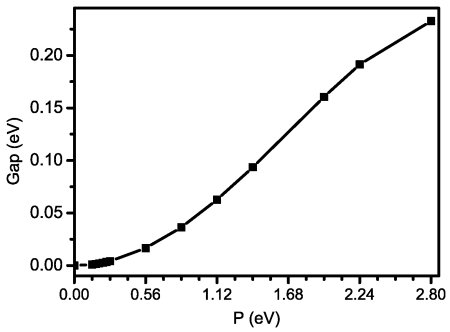

Fig. 5 The change in the magnitude of band gap opening with increasing on-site energy P (eV) for graphene.

We then investigate the effect of change in the hopping integral without consideration of the on-site energy change. Fig. 6(a) demonstrates the dependence of the band gap on Δt, the amplitude of the charge hopping integral on account of the bond length variation. For all the distortion configurations considered here, there is a visible band gap opening. As a result of C–C bond length variations, in graphene, the k-point at which band gap opening occurs (the gap point) undergoes a shift in the cases of distortion configurations d2, d3 and d4. The distortion pattern assumed in configuration d1 has a threefold symmetry, similar to pristine graphene. As a result, in this case, the gap point does not undergo a shift, in variance with the three other configurations. Fig. 6(b) shows the shift of gap point for d2 and d3 configurations, which reflects the band gap variations. The gap point shift thus translates into a regular variation of the band gap about a mean value for all the configurations considered, except d1.

We further consider the effect of the on-site energy in the presence of a constant finite value of Δt. Fig. 7(a) illustrates the band gap variation as a function of P when $\Delta t = 0.5\% t$. All the distortion forms follow a similar trend, in which the band gap is first reduced and then increases. The effect of the two parameters, Δt and P, on the band gap is of subtly competing nature. A larger Δt implies a shortening of the C–C bond

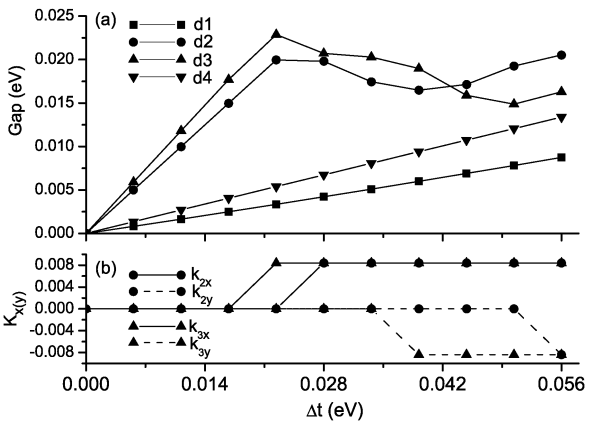

Fig. 6 (a) The change in the magnitude of band gap opening with the amplitude of the charge hopping integral (Δt) for all the distortion configurations of graphene. (b) The change in the K point with increasing (Δt), corresponding to the configurations d2 and d3.

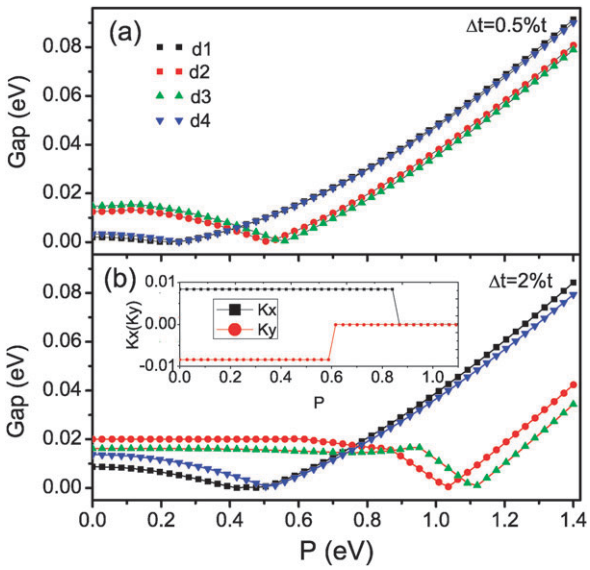

Fig. 7 The effect of increasing the on-site energy P (eV) on the band gap opening for the four distorted graphene configurations with Δt kept constant at (a) $0.5\% t$ and (b) $2\% t$.

length, and hence a corresponding increase in the charge hopping integral opens up the band gap of graphene.

An increase in the on-site energy, P, implies a higher potential ascribed at the sites of the carbon atoms of graphene sandwiched by pyrene (illustrated by blue circles in Fig. 4). The sites in graphene that correspond to the atoms not sandwiched by pyrene do not acquire a change in P. This may result in a decrease of the hopping integral between a sandwiched carbon atom of graphene and its nearest neighbor C-atom if the latter is located in the unsandwiched area of the graphene sheet.

Although an increase in both Δt and P yields a larger band gap, a comparison of Fig. 5 and Fig 6(a) reveals that the effect of Δt is about an order of magnitude larger than that of P. The dominance of Δt, combined with its competing tendency to the influence of P on the band gap, results in an insignificant change in the band gap upon an initial increase of P. As P is increased further, the gap gradually reaches a minimum, at which point both effects counterbalance each other. Band gap widening is observed for further increases in P. As shown in Fig. 7(b), a higher $\Delta t = 2\% t$ causes the band gap opening to remain insensitive to a larger initial increase in P from zero. The inset of Fig. 7 depicts the shift in the gap point with increasing P for the d2 configuration when Δt is $2\% t$.

As the band gap opening is shown to be dependent upon P and Δt, the combined effect of both needs to be evaluated. Fig. 8 demonstrates the widening of the band gap by the simultaneous influence of P and Δt for all the distortion configurations of graphene. The largest band gap opening is observed in the regime of a large P value. The aforementioned competing effects of P and Δt lead to a trough-like feature in all the graphs.

The upper limit values of the on-site energy considered for the sake of the calculations here may not represent a realistic case. To imitate a possible practical implementation of pyrene-adsorbed graphene more accurately, we chose the values of

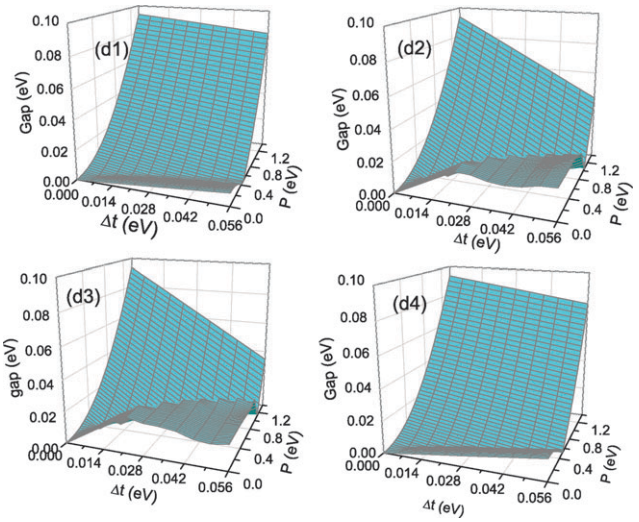

Fig. 8 Band gap opening with increasing on-site energy P (eV), and the change in the hopping integral (Δt) for the four distorted graphene configurations d1, d2, d3 and d4, as indicated in the respectively-labelled plots.

Δt and P as 0.0056 and 0.56 eV, respectively. The value of Δt = 0.0056 eV (0.2%t) is chosen as the same order as the maximum percentage change observed in the C–C bond length in pyrene-dispersed graphene. The energy band diagram and the corresponding density of states are calculated for all the four distortion configurations. Fig. 9(a)–(d) depict the band structure for distortion configurations d1–d4, respectively, while the corresponding density of states profiles are plotted in Fig. 9(e)–(h). We observe the band gap opening from 10.1 to 15.3 meV for the d3 and d1 distortion configurations, respectively.

The actual magnitude of band gap opening depends upon the underlying working mechanism. Graphene with tetracyanoethylene (TCNE) adsorbed physically onto it was shown to exhibit a band gap of 40 meV at low density.[21] The difference from our results is possibly due to the consideration of weak charge-transfer from graphene to TCNE by Lu *et al.*[21] Furthermore, the bond-structure distortions in graphene observed by us are much smaller, which may also represent the smaller magnitude of the band gap opening. In general, chemical adsorption and charge-transfer between graphene and the adsorbate can be expected to have a greater effect on band gap opening. Balog *et al.* have reported recently a band gap of up to 450 meV in graphene exposed to atomic hydrogen.[19] Their reported upper limit of band gap opening is much larger than that presented in this paper. However, the nature of the experiment suggests that by lowering the extent of hydrogen adsorption onto graphene, band gap tunability towards smaller values may become possible. Furthermore, within the scope of our current work, the influence of only the physical adsorption of pyrene on graphene is studied. It is important to note that similar effects on the opening of the band gap may be expected if the nature of the adsorption is chemical. Suitable species may strongly interact with graphene *via* formation of covalent bonds.[30,31] For such systems also, *ab initio* studies have revealed the possibility of a distinct band gap opening.

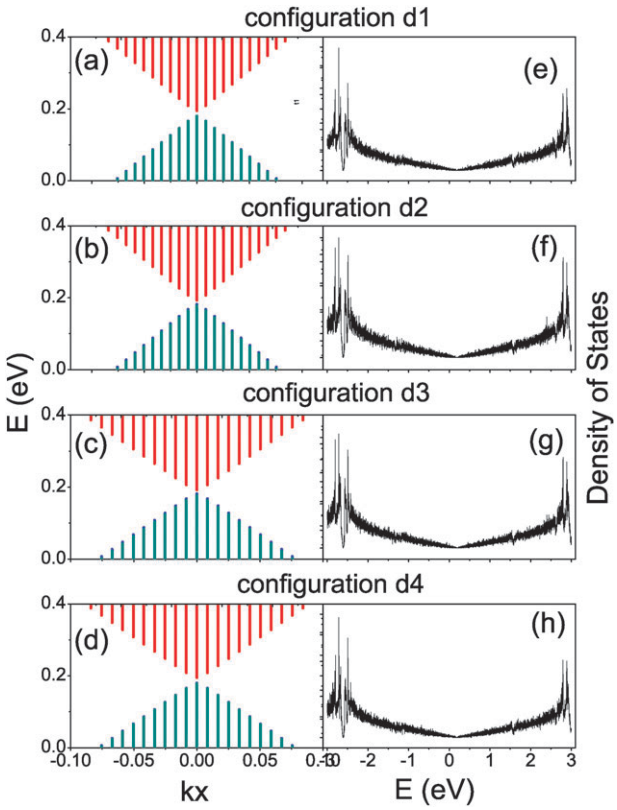

Fig. 9 Energy band structures for all four distortion configurations of graphene, d1–d4 ((a)–(d)). A small band gap opening can be observed in each case. (e)–(h) denote the corresponding density of states' profiles for configurations d1–d4, respectively. The calculations are performed at Δt = 0.0056 eV and P = 0.56 eV.

4. Conclusions

In summary, we have studied the electronic structure and characteristics of pyrene-adsorbed graphene. Different configurations of bond length distortions in graphene due to the adsorption of pyrene are formulated based on DFT results. We have employed the tight binding model to examine the band gap behavior of graphene. We show that all the configurations exhibit a small band gap opening as a function of charge hopping integral modification (Δt) and the on-site energy (P). Our results thus support the assertion that the bond length distortions lead to a breakdown of the sublattice symmetry in graphene, thereby opening up a band gap.

With Δt = 0.0056 eV (0.2%t) and P = 0.56 eV (20%t) representing a set of parameter values in a practical scenario, band gap opening is observed in the order of 10 meV. The obtained magnitude of the band gap width is comparable to that reported in previous studies examining effects of adsorbate species, such as hydrogen or organic molecules such as TCNE, at the lower limits of adsorption. We thus demonstrate that graphene can be made suitable for electronic device applications *via* the adsorption of pyrene in a periodic fashion. Furthermore, our approach of bandstructure study, by employing a modified charge-transfer integral, can be applied to other graphene systems involving interactions with deposited species. In particular, efforts in the electronic structure explorations of different

GICs could benefit from our approach of evaluating electronic properties.

Acknowledgements

Support from the Singapore Ministry of Education through the Academic Research Fund (Tier 2) under Project no. T207B1214 and from the National Nature Science Foundation of China (Grant no. 10947125) is gratefully acknowledged. The authors thank Jun Ye for assistance.

References

1 K. S. Novoselov, A. K. Geim, S. V. Morozov, D. Jiang, Y. Zhang, S. V. Dubonos, I. V. Grigorieva and A. A. Firsov, *Science*, 2004, **306**, 666.
2 C. Berger *et al.*, *J. Phys. Chem. B*, 2004, **108**, 19912.
3 R. Saito, G. Dresselhaus and M. S. Dresselhaus, *Physical properties of Carbon Nanotubes*, Imperial College Press, London, 1998.
4 A. H. Castro Neto, F. Guinea, N. M. R. Peres, K. S. Novoselov and A. K. Geim, *Rev. Mod. Phys.*, 2009, **81**, 109.
5 J. Hass, R. Feng, T. Li, X. Li, Z. Zong, W. A. de Heer, P. N. First, E. H. Conrad, C. A. Jeffrey and C. Berger, *Appl. Phys. Lett.*, 2006, **89**, 143106.
6 X. Li, X. Wang, L. Zhang, S. Lee and H. Dai, *Science*, 2008, **319**, 1229.
7 G. Giovannetti, P. A. Khomyakov, G. Brocks, P. J. Kelly and J. V. D. Brink, *Phys. Rev. B: Condens. Matter Mater. Phys.*, 2007, **76**, 073103.
8 S. Y. Zhou, G. H. Gweon, A. V. Fedorov, P. N. First and W. A. Heer, *Nat. Mater.*, 2007, **6**, 770.
9 E. V. Castro, K. S. Novoselov, S. V. Morozov, N. M. R. Peres, J. M. B. Lopes dos Santos, J. Nilsson, F. Guinea, A. K. Geim and A. H. Castro Neto, *Phys. Rev. Lett.*, 2007, **99**, 216802.
10 Y. Zhang, T.-T. Tang, C. Girit, Z. Hao, M. C. Martin, A. Zettl, M. F. Crommie, Y. R. Shen and F. Wang, *Nature*, 2009, **459**, 820.
11 J. Bai, X. Zhong, S. Jiang, Y. Huang and X. Duan, *Nat. Nanotechnol.*, 2010, **5**, 190.
12 J. Berashevich and T. Chakraborty, *Phys. Rev. B: Condens. Matter Mater. Phys.*, 2009, **80**, 033404.
13 W. Liu, Z. F. Wang, Q. W. Shi, J. Yang and F. Liu, *Phys. Rev. B: Condens. Matter Mater. Phys.*, 2009, **80**, 233405.
14 T. G. Pedersen, C. Flindt, J. Pedersen, N. A. Mortensen, A.-P. Jauho and K. Pedersen, *Phys. Rev. Lett.*, 2008, **100**, 136804.
15 J. O. Sofo, A. S. Chaudhari and G. D. Barber, *Phys. Rev. B: Condens. Matter Mater. Phys.*, 2007, **75**, 153401.
16 L. Liu and Z. Shen, *Appl. Phys. Lett.*, 2009, **95**, 252104.
17 D. C. Elias *et al.*, *Science*, 2009, **323**, 5914, 610.
18 J. Zhou, M. M. Wu, X. Zhou and Q. Sun, *Appl. Phys. Lett.*, 2009, **95**, 103108.
19 R. Balog, B. Jorgensen and L. Nilsson *et al.*, *Nat. Mater.*, 2010, **9**(4), 315–319.
20 W. Chen, S. Chen, D. C. Qi, X. Y. Gao and A. T. S. Wee, *J. Am. Chem. Soc.*, 2007, **129**(34), 10418.
21 Y. H. Lu, W. Chen, Y. P. Feng and P. M. He, *J. Phys. Chem. B*, 2009, **113**, 2.
22 X. Dong, D. Fu, W. Fang, Y. Shi, P. Chen and Lain-Jong Li, *Small*, 2009, **5**, 1422.
23 X. Dong *et al.*, *Phys. Rev. Lett.*, 2009, **102**, 135501.
24 M. Vanevic, V. M. Stojanovic and M. Kindermann, *Phys. Rev. B: Condens. Matter Mater. Phys.*, 2009, **80**, 045410.
25 N. Vukmirovic, V. M. Stojanovic and M. Vanevic, *Phys. Rev. B: Condens. Matter Mater. Phys.*, 2010, **81**, 041408.
26 T. Valla, J. Camacho, Z.-H. Pan, A. V. Fedorov, A. C. Walters, C. A. Howard and M. Ellerby, *Phys. Rev. Lett.*, 2009, **102**, 107007.
27 N. Emery, C. Herold, M. dAstuto, V. Garcia, Ch. Bellin, J. F. Mareche, P. Lagrange and G. Loupias, *Phys. Rev. Lett.*, 2005, **95**, 087003.
28 M. P. M. Dean, C. A. Howard, S. S. Saxena and M. Ellerby, *Phys. Rev. B: Condens. Matter Mater. Phys.*, 2010, **81**, 045405.
29 Z.-H. Pan, J. Camacho, M. H. Upton, A. V. Fedorov, A. C. Walters, C. A. Howard, M. Ellerby, T. Valla, arXiv:1003.3903v1.
30 I. Zanella, S. Guerini, S. B. Fagan, J. Mendes Filho and A. G. Souza Filho, *Phys. Rev. B: Condens. Matter Mater. Phys.*, 2008, **77**, 073404.
31 E. J. G. Santos, A. Ayuela, S. B. Fagan, J. Mendes Filho, D. L. Azevedo, A. G. Souza Filho and D. Sánchez-Portal, *Phys. Rev. B: Condens. Matter Mater. Phys.*, 2008, **78**, 195420.

